Materials Science & Engineering C 99 (2019) 957–968

Contents lists available at ScienceDirect

Materials Science & Engineering C

journal homepage: www.elsevier.com/locate/msec

Soybean-modified polyamide-6 mats as a long-term cutaneous wound covering

Fernanda Trindade Gonzalez Dias[a,*], Anderson Ricardo Ingracio[b], Natália Fontana Nicoletti[c], Felipe Castro Menezes[d], Lucas Dall Agnol[b], Daniel Rodrigo Marinowic[e], Rosane Michele Duarte Soares[d], Jaderson Costa da Costa[e], Asdrubal Falavigna[b,c], Otávio Bianchi[a,b]

[a] Materials Science Graduate Program (PGMAT), Universidade de Caxias do Sul (UCS), Caxias do Sul, RS, Brazil
[b] Health Sciences Graduate Program, Universidade de Caxias do Sul (UCS), Caxias do Sul, RS, Brazil
[c] Cell Therapy Laboratory (LATEC), Universidade de Caxias do Sul (UCS), Caxias do Sul, RS, Brazil
[d] Poli-BIO, Polymeric Materials Research Group, Institute of Chemistry, Universidade Federal do Rio Grande do Sul, Porto Alegre, RS, Brazil
[e] Brain Institute of Rio Grande do Sul (BraIns), Pontifícia Universidade Católica do Rio Grande do Sul (PUCRS), Porto Alegre, RS, Brazil

ARTICLE INFO

Keywords:
Wound healing
Polyamide-6
Nanomembrane
Electrospinning
Cytotoxicity
Growth factor

ABSTRACT

Engineered skin coverings have been adopted clinically to support extensive and deep wounds that result in fewer healthy skin remaining and therefore take longer to heal. Nonetheless, these biomaterials demand intensive labor and an expensive final cost. In comparison to conventional bandages, which do not meet all the requirements of wound care, electrospun fiber mats could potentially provide an excellent environment for healing. In this work, we developed two nanostructured scaffolds based on polyamide-6 (PA-6) to be tested as a wound covering in a rat model of full-thickness incisional wound healing. The central idea was to create a bioconstruct that is simple to implement and biologically safe, with a high survival rate, which provides physical support and biological recognition for new functional tissues. An unmodified PA-6 and a soybean-modified PA-6 were employed as nanofibrillar matrices in this study. The biomaterials showed a dimensional homology to natural extracellular matrix components and neither *in vitro* toxicity nor *in vivo* side effects. Both polymeric scaffolds were resistant to the sterilization process and could promote the attachment of 3T3 fibroblast cells, besides successfully incorporating the growth factor PDGF-BB, which had its bioactivity extended for up to 12 h under simulated conditions. The modification of PA-6 chains with a fatty acid derivative increased the scaffold's surface free energy, favoring cell proliferation, collagen formation, and ECM secretion. These results confirm the potential of these materials as a topical dermal covering for skin regeneration.

1. Introduction

In the last decade, temporary and permanent bioengineered wound covering for hard-to-heal injuries have made significant gains with advancing technology in biomaterials and tissue engineering [1,2]. The cost to manage these wounds is likely to increase by $33 billion over the next ten years [3]. Most researches focus on developing degradable biomaterials with short-term use, and only a few works report the long-term implantation of materials intended for the treatment of severe skin wounds, such as those from diabetic ulcers or third-degree burn [4,5]. The difficulty that these wounds have to heal spontaneously may be due to the lack of support to guide cell growth, reduced levels of endogenous growth factors, and blood vessel maturation [6]. Patients with these conditions cannot endure procedures involving a large extent of the skin surface, and their treatment relies on simple surgical dressing to alleviate the physical symptoms (such as exudate, pain, and bleeding) and regenerate wound areas [7].

The objective of this study was to design a long-term wound covering for deep or persistent cutaneous injuries, capable of meeting some performance requirements: three-dimensional mimetic morphology; easily handling and light-weight; conformable to irregular surfaces; long-term biocompatible and non-toxic; good fluid retention and exudate control; mechanical resistance to serve as barrier protection and support tissue ingrowth, avoiding scarring and not impairing re-epithelialization; and affinity with biomolecules that stimulates angiogenesis and cell proliferation at early stages of healing [8]. These long-

* Corresponding author.
E-mail address: ftgdias@ucs.br (F.T.G. Dias).

https://doi.org/10.1016/j.msec.2019.02.019
Received 20 February 2018; Received in revised form 10 October 2018; Accepted 6 February 2019
Available online 08 February 2019
0928-4931/

term biomaterials could be an alternative in circumstances when standard therapies for treating persistent wounds are not efficient. Conventional dressings do not provide a matrix for cell infiltration, proliferation, and extracellular matrices (ECM) remodeling [9]. Long-term wound coverings would act as a protective layer template between the wound bed and the new tissue formed, ensuring a better permanently healing. As long as the biomaterial was slowly degraded, the new tissue would be allowed to grow into the nanofibrous material interstices, being assimilated by the body and acting as an ECM [10]. Moreover, there would be no need for frequent dressing changes, diminishing patient's discomfort and wound exposure to external pathogens [4].

In this context, nanomembranes produced by the electrospinning technique could potentially provide an excellent environment for healing [11]. Nonwoven membranes have three-dimensional interconnected pore networks and a high surface area [12,13]. Also, these constructs are structurally similar to ECM in biological tissue, which is ideal for cellular attachment and proliferation [14–16]. Electrospun scaffolds can further be impregnated with antibacterial and biological agents, thus improving cell compliance, and tissue regeneration [11,16,17]. Peptide nanofibers provide synthetic platforms to reconstruct both morphological characteristics and bioactive properties of cellular microenvironments [18]. Polyamides are structurally similar to proteins, and their breakage can produce free amine and carboxylic acid derivatives [19]. The hydrolytic degradation of a polyamide-6 (PA-6) based implant under physiological conditions (pH ~7.0 and 37 °C) starts by the second week after intervention, and 15–20% is degraded per year [20–22]. In contrast, poly(lactic acid) (PLA), a commonly chosen biodegradable polymer for dressings, loses 75% of its weight in < 40 days when immersed in buffer solutions [19,23]. In the case of polyamides, the mat degradation rate can be tunable, respecting the patient's needs and causing minimal impact on the surrounding tissues [11,24,25]. Electrospun polyamide nanofibers can offer hydrophilic surface, good mechanical strength, and suitable biocompatibility as ideal properties for skin wound healing [12,13,15].

In this work, we developed two electrospun scaffolds based on PA-6 to be investigated as an *in vivo* sacrificial substrate for the epithelialization of wounds. An unmodified PA-6 and a maleinized soybean modified PA-6 (PA-6/SOMA) were employed as nanofibrillar matrices in this study. The soybean oil presented in SOMA has a source of essential fatty acids and tocopherols, related to antioxidant and anti-inflammatory and epithelizing properties. Soy thermoplastics materials were found to be noncytotoxic and even encouraged cell proliferation during *in vitro* tests [26]. We hypothesized that wound coverings produced from PA-6/SOMA might contribute to better tissue regeneration for support handling and cellular morphogenesis. To evaluate the PA-6 nanomembranes with respect to further applications, this work investigated (1) the microstructure of the electrospun biomaterials, (2) their morphology characteristics, (3) their wettability and fluid retention capacity, (4) their interaction with bioactive molecules, (5) their cytotoxicity and adhesion behavior in the presence of 3T3 and VERO cell cultures, and (6) their behavior when in direct contact with an *in vivo* wound microenvironment. It is expected that these nanomembranes adhere and provide a skin barrier to the wound long enough to promote healthy healing [27].

The scarcity of long-term synthetic coverings available in the market hampers a broad comparison with the material proposed in this study. Among the nylon-based biomaterials produced for long-term use are the commercials Biobrane®, Mepitel®, and Silverlon®. These products are examples of polyamide silicon membranes approved as synthetic skin substitutes [4,28–31]. However, despite being expensive and difficult to manipulate and apply, these materials have been associated with wound contraction and permanent scarring in partial-thickness scald wounds. Advances in nanotechnology and biomedical sciences must be continually encouraged to improve techniques and procedures for skin regeneration and repair.

2. Materials and methods

2.1. Materials

PA-6 resin (RADILON S40F) (M_v: 53,000 $gmol^{-1}$) was donated by Mantova Plastic Tubes Company (Caxias do Sul, Brazil). The PA-6/SOMA (M_v: 66,000 $gmol^{-1}$) sample was produced by the reaction of PA-6 chains with 5 wt% of maleinized soybean oil (SOMA) in a co-rotating twin-screw extruder, according to the literature [32]. Formic acid 85% v/v purchased from Neon Comercial (São Paulo, Brazil) was used as a solvent without further purification. VERO (kidney epithelial cells of African green monkey) and 3T3 (murine fibroblast) cell lines were from American Type Culture Collection (ATCC-Rockville, Maryland, USA). The recombinant human platelet-derived growth factor (rhPDGF-BB) was purchased from Pepro Tech Inc. (Rocky Hill, NJ).

2.2. Nanomembrane production and characterization

The nanofibrous mats were prepared by an electrospinning apparatus (INSTOR, Porto Alegre, RS) from solutions of PA-6 and PA-6/SOMA in formic acid. Different electrospinning conditions and concentrations of polymeric solutions were tested on fiber production (see in Supplementary files, Table S1). Defect-free membranes were obtained from 32 wt% solutions at a feeding rate of 0.1 mL/h, using a syringe-collector distance of 15 cm and an applied voltage of 25 kV. The electrospinning process was carried out at room temperature. ATR-FTIR analyses were used to verify the presence of residual formic acid by the 1727 cm^{-1} band, and no solvent trace was found in the fibrous mats (result not shown). The nanofiber morphology was evaluated by a field-emission scanning electron microscope Mira 3 Tescan (FEG-SEM) (Czech Republic). Samples were coated with gold using a plasma sputtering apparatus for FEG-SEM analysis. For each sample, at least 50 fibers were manually measured and analyzed using ImageJ software (NIH, USA). The average fiber diameters were expressed as mean standard deviation [33].

The Wide-Angle X-ray Diffraction (WAXD) pattern of the electrospun mats was investigated to obtain information about the microstructure of materials. The analyses were performed at 20 °C using a Shimadzu XRD-6000 diffractometer. Scans were carried out from 3° to 40° (2θ) at a scan rate of 2θ/min using Cu-Kα radiation. The diffractograms were mathematically treated to estimate the relative fractional crystallinity and the amount of γ-form polyamide crystals. The lamellar structure of the materials was evaluated using small-Angle X-ray Scattering (SAXS) experiments. The experiments were performed on the SAXS1 beamline of the Brazilian Synchrotron Light Laboratory (LNLS), using a Pilatus detector (300 k Dectris) positioned at 836 mm and scattering wave vectors (q) from 0.13 to 2.5 nm^{-1}. The wavelength of the incident X-ray beam was 0.155 nm.

The surface free energy of the PA-6 and PA-6/SOMA samples was determined by the Owens–Wendt method, which is based on contact angle measurements conducted with certain measuring liquids [34,35]. Although it cannot be assumed that the surface properties of electrospun mats are similar to those of bulk, the wettability behavior of the pristine solid specimens will already allow us to predict the hydrophilicity of these nanomembranes [35]. The contact angle measurements were carried out in an SEO® Phoenix100 (Korea) equipment and five probe liquids were employed: distilled water (γ_L^P = 51.0 mJ/m^2; γ_L^D = 21.8 mJ/m^2; γ_L = 72.8 mJ/m^2), glycerin (γ_L^P = 29.7 mJ/m^2; γ_L^D = 33.6 mJ/m^2; γ_L = 63.3 mJ/m^2), dimethyl sulfoxide (γ_L^P = 8.0 mJ/m^2; γ_L^D = 36.0 mJ/m^2; γ_L = 44.0 mJ/m^2), n-hexadecane (γ_L^P = 0.0 mJ/m^2; γ_L^D = 27.6 mJ/m^2; γ_L = 27.6 mJ/m^2) and bovine serum albumin (BSA) aqueous solution (1 g/dl) (γ_L^P = 2.5 mJ/m^2; γ_L^D = 38.3 mJ/m^2; γ_L = 40.8 mJ/m^2); where γ_L^P, γ_L^D and γ_L represent the polar component, the dispersive component and the surface free energy of the liquids, respectively [36,37]. The sessile drop method was adopted using 2 μL drops. The contact angle was measured at least ten

times at different sites on the surface, the average value being considered.

The fluid uptake capacity of the nanomembranes was examined by their submersion in phosphate-buffered saline (PBS) solution of pH 6.0 at 37 °C. At predetermined time intervals, the samples were taken out of the buffer solutions, and the amount of fluid absorbed was weighted. The excess of buffer on the surface of wet samples wiped dry with filter paper. The fluid uptake capacity (wt%) of the nanomembranes was determined as follows:

$$\textit{Fluid uptake capacity}\ (\text{wt\%}) = \left(\frac{W - W_d}{W_d}\right) * 100 \quad (1)$$

where W is the weight of wet nanofiber sample at time and W_d is the initial weight of the sample in its dry state before submersion in PBS solution.

2.3. PA-6 nanomembranes as wound covering materials

2.3.1. Affinity and association with biomolecules

To evaluate the attachment of peptides to the nanofibrillar surfaces, PDGF-BB was used. The growth factor (GF) was reconstituted in 0.1% BSA and diluted with ultra-pure water to achieve a concentration of 10 μg/mL and stored at −80 °C. PDGF-BB (100 ng/mL) in solution was added to PA-6 and PA-6/SOMA nanomembrane surfaces and incubated for 45 min at 37 °C. The GF attachment to the membrane was assessed by ATR-FTIR and FEG-SEM.

The PDGF-BB release from PA-6 electrospun nanofibers was preliminarily investigated. Twenty microliter of PDGF-BB solution (200 ng) was directly applied on PA-6 mats of 1 cm^2 with a micropipette. The solution was taken up entirely at 37 °C for 45 min by the initially dry nanomembranes. PDGF-BB had not been chemically conjugated, but directly embedded onto PA-6 scaffolds. Each sample was then placed into a tube containing 4 mL of PBS 1× (pH 6.0) and kept on an orbital shaker at 37 °C. At predetermined time points over a period of 5 days, 200 μL of PBS solution was collected for later analysis (20 °C) and replenished with 200 μL fresh PBS. The cumulative amount of PDGF-BB in the release media from each sample was measured using a human PDGF-BB enzyme-linked immunosorbent assay (ELISA) kit (RayBiotech, Catalog #ELH-PDGFBB, Norcross, GA) ($N = 2$ for each group per time points), according to the manufacturer instructions. The optical density of the developed color was measured using a microplate reader at 450 nm (iMark Microplate Reader, Bio-Rad Laboratories, Hercules, CA).

2.3.2. In vitro cytotoxicity and cellular adhesion

VERO and 3T3 cells were cultured in Dulbecco's Modified Eagle Medium with 10% fetal bovine serum (FBS) at a temperature of 37 °C, minimum relative humidity of 95%, and an atmosphere of 5% CO_2 in air. PA-6 nanofibrous mats ($N = 3$ per group per experiment) were sterilized under 120 mm Hg pressure for 45 min and subsequently dried at 37 °C for seven days. The cell lines were incubated with commercial PA-6 and PA-6/SOMA nanomembranes by direct contact and elution methods at a size corresponding to 3 cm^2/mL, as recommended by ISO 10993 [38]. All experiments were performed three times in triplicate. To assess cell viability, the metabolically active mitochondria were evaluated by MTT assay at 24 h, 48 h, and 72 h. Data from *in vitro* experiments were analyzed by one-way analysis of variance (ANOVA) followed by Bonferroni's post-hoc test, using Graph-Pad Software (San Diego, CA, U.S.A.). $P < 0.05$ was indicative of statistical significance.

To verify cell adhesion, the materials were held in the deep 24-well plate, and the cells were seeded on the membranes at the density of 15–20 × 10^3 cells per well, and cultured for 24 h or 72 h. The cells were fixed with 2.5%vol. glutaraldehyde, and sequentially dehydrated in increasing concentrations of ethanol (50, 70, 85, 95 and 100%). The samples were left for 1 h in 100% ethanol and allowed to air dry at room temperature. Cell morphology and adhesion were assessed by SEM results.

2.3.3. In vivo wound healing evaluation

Wistar albino male adult rats (8 weeks old, 250–300 g; total $N = 37$) were used to evaluate the *in vivo* dressing by a wound healing model. The animals were housed under conditions of optimum light, temperature and humidity (12 h light-dark cycle, 22 ± 1 °C, under 60 to 80% humidity), with food and water provided *ad libitum*. The Federal University of Rio Grande do Sul supplied the animals (UFRGS, Brazil). All the experimental procedures were under the Principles of Laboratory Animal Care from NIH, and were approved by the local Animal Ethical Committee (CEUA-UCS; protocol number: 015/2016).

Two incisional full-thickness circular wounds (1 cm in diameter) were made on the upper back of each animal using a sterile punch. The animals were previously anesthetized by an intraperitoneal administration of ketamine and xylazine (80 and 10 mg/kg, respectively). Equal areas of the wound sizes were treated with either control (untreated wound) or commercial PA-6 or PA-6/SOMA (loaded with GF or not) membranes placed inside the injury, not sutured to the skin ($N = 6$ animals/group; Total $N = 36$). After recovery from anesthesia, the animals were placed in individual cages, and the wound sites were observed macroscopically throughout 14 days. An animal ($N = 1$) was used to evaluate the nanofibrillar surface of PA6-SOMA (loaded with GF or not) after 3 days within the wound. Microscopic evaluation of cell content on the nanofibrillar surface was made by FEG-SEM.

3. Results and discussion

3.1. Morphological and structural properties of polyamide-6 nanomembranes

Fig. 1 shows the morphological appearance of the produced electrospun scaffolds. The processing parameters influenced fiber formation during electrospinning, among which viscosity of the polymeric solution was vital to spinnability and fiber morphology [17]. The PA-6 and PA-6/SOMA fibrous mats (Fig. 1a and b) were composed of uniform, random and free-globular fibers and exhibited average diameters of 171.0 ± 11.0 nm and 250.0 ± 9.0 nm, respectively. The PA-6/SOMA slightly increased the average diameter of the fibers, mainly due to the molecular weight of the modified polymer [16]. Interestingly, these diameter values are within range of extracellular matrix collagen fibers (ECM) (50–500 nm) [15].

This is a good starting point toward the development of a synthetic scaffold able to reproduce the natural structure of ECM [39]. Besides, a sterile biomaterial is necessary to prevent wound contamination and subsequent infection [40]. In this regard, these nanomembranes were able to withstand an autoclave sterilization process (120 mm Hg/45 min), showing that the aseptic process did not affect the structural integrity of PA-6 nor the average diameter of the fibers (Fig. 1c and d).

The effect of polymer processing and its impact on structural conformation is essential to understand the material property. For example, changes in the structure of the crystal phase and the crystal size might directly impact on the physicomechanical characteristics of polymers as well as their biological response [41–43]. Not only the chemical architecture of the fiber is outstanding, but its ability to form a 3D network which promotes cellular activity. In this context, the electrospinning process effect on nylon-6 chain conformation and crystal structure should be investigated. The WAXD analysis elucidates the structure/property/process relationships in electrospinning, making it possible to understand the microstructure developed during fiber formation [44]. PA-6 is a polymorphic material, having more than one energetically favorable crystalline phase such as α and γ-forms [43]. The α form of PA-6 usually exhibits two characteristic reflections around 20.3° and 23.8° (2θ) whereas the γ form presents a distinctive reflection at 21.6° (2θ) [45–47]. The three crystalline phases were

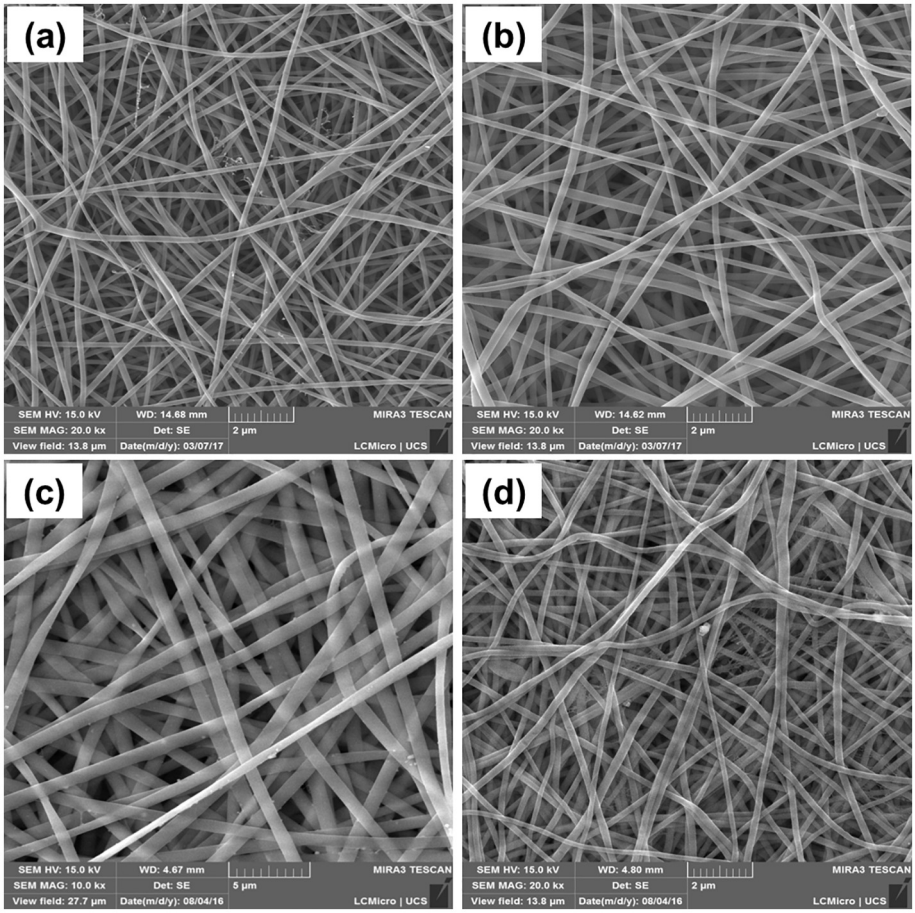

Fig. 1. Morphological appearance (FEG-SEM) of electrospun materials at 32 wt%: (a) commercial PA-6; (b) PA-6/SOMA; (c) sterilized commercial PA-6 and (d) sterilized PA-6/SOMA.

detected in the pre-electrospun PA-6/SOMA diffractogram (see Supplementary data, Fig. S1) [32]. For the other samples, the diffraction patterns revealed a single peak at about 21° (2θ). Little is known about the crystalline structures and their transitions in PA-6 electrospun nanofibers. For this polymer, the free energies of the α and γ-forms are relatively close to each other, which allows the interconversion between these forms upon the use of certain solvents or experimental conditions [41,42].

Quantitatively, peak deconvolution was used to estimate the fractional crystallinity and the amount of γ-form crystals (see Supplementary data, Table S2). The relatively amorphous and crystalline phases were computed according to the procedure developed by Brian P. Grady [48], which fits the crystalline peaks and amorphous halo through a Gaussian–Lorentzian area function. The results indicated that the electrospinning process led to a crystallinity reduction when compared to the solid samples [46]. This can be justified by the high stress applied during fiber formation in the electrospinning process, which does not allow for the necessary time for crystallization to develop [42,43,45]. The amount of γ-phase also decreased from the solid samples to the electrospun fibers. The development of γ-form crystals in as-spun fibers occurs preferably in solutions with low polymer contents (4–12 wt%) whereas, at higher concentrations (as in our case), this phase content is gradually reduced [47]. Since there is a substantial overlap between the positions of the amorphous and crystalline peaks, the fitted parameters should only be used to compare the samples within this experiment in qualitative trends [49].

PA-6 and PA-6/SOMA materials showed a typical I(q) *vs.* $q^{-3.7}$ in SAXS curves (see Supplementary files, Fig. S2), which it is characteristic of fibrillar structures elongated in one direction [35,42,44,50]. The nanomembranes showed a reduction in the lamellar long period from ~10 nm to 5.7 nm, due to the orientation of polymer chains during the electrospinning process. The elongation force during the electrospinning process dramatically influences the macromolecular assemblies within the fibers, in particular, their macromolecular orientation, chain conformation, and crystal structure [44]. The nonwoven electrospun mats revealed isotropic strong diffuse scattering near the beam stop, which can be attributed to nanofibrils or microvoids within these nanostructures [44,50]. The 2D SAXS patterns for the electrospun scaffolds exhibited a circumferential shape representing the lack of structural alignment along the fiber axis as well as the scattering from fibers in all directions [44,51,52].

For biomaterials applications, the adhesion phenomenon plays a significant role. Thus the surface free energy must be investigated through its dispersive and polar components [34,35]. The biological molecules affinity for a 3D scaffold is profoundly affected by the nature of the biomaterial surface [35]. Increased nanomembrane wettability also improves implant tissue integration [53]. The Owens-Wendt theory determines the polar and dispersive contributions to a solid's surface free energy using the known polar and dispersive components of the probe liquids and their contact angles with the solid (see Supplementary data, Table S3) [35]. The total surface free energy of the PA-6 solid sample was 47.5 mN/m, which is in agreement with the literature values [5,35]. The PA-6/SOMA has contributed to the increase of surface free energy, which favors adhesiveness energetically and might help obtain a cell response. The higher the surface free energy value, the higher the wettability and bioactivity of a biomaterial. From the contact angle results with n-hexadecane, it is clear that the chemical modification has made PA-6/SOMA material moderately hydrophilic. Many

studies have demonstrated that cells adhere, spread and grow more readily on moderately hydrophilic substrates than on hydrophobic or very hydrophilic ones [5,6]. The PA-6/SOMA sample also presented higher affinity with BSA solution, confirming a more pronounced interaction with the protein molecules. The association of long-chain fatty acids with BSA has a physiological significance since albumin is the principal vehicle for free fatty acid (FFA) transport through the plasma. The association of FFA with albumin is thought to involve electrostatic attraction of the FFA carboxyl group to protein cationic sites together with hydrophobic interactions between the FFA hydrocarbon tail and nonpolar side chains of the protein [54].

The swelling degree of the bulk PA-6 polymer in water is approximately 10 wt% [55–57]. The PA6-based nanowebs created by electrospinning were able to retain a large amount of interstitial fluid when in direct contact with a PBS solution of pH 6.0 at 37 °C (see Supplementary data, Fig. S3). A remarkable fluid absorption was observed for both nanostructures, which were able to absorb about 700% of PBS with only 1 h immersion. This can be explained by the high surface area to volume ratio of these nanoconstructs, with interconnected three-dimensional voids that may facilitate fluid infiltration [58,59]. Certainly, this behavior can also be related to the hydrophilic nature of the polymer itself [60]. An ideal wound biomaterial should maintain a moist environment to promote autolytic debridement, prevent the wound bed dehydration and accumulation of exudates [61]. Autolytic debridement often results in the production of large quantities of enzyme- and nutrient-rich wound fluid during the first treatment week [62]. Wounds with moderate to high exudate include large venous ulcers and ulcerative cutaneous condition, which benefit from covering with great absorptive capacities that also minimize maceration of surrounding healthy skin. The moisture also allowed the fast polyamide adherence into the wound bed and contributed to biomaterial integration at the injury site, as well as to the permeability of oxygen and diffusion of therapeutic molecules [63]. It is important to highlight that this absorbent feature made the polyamide mats easy to be appropriately removed by the local soaked in sterile water or saline when changes are needed, with minimal pain or trauma to the wound bed [64].

3.2. Nanomembrane interaction with the PDGF-BB growth factor

The development of bio-active matrices from scaffolds embedded with growth factors can provide the necessary biological recognition in the wound healing process [17]. The affinity of a recombinant human PDGF-BB by the nanofibrillar surfaces was evaluated for the purpose of stimulating cell-material interactions. The nanofibrous scaffolds successfully loaded PDGF-BB. The incorporation of this biomolecule to the PA-6/SOMA nanomembrane was confirmed by FEG-SEM and FTIR results [17,65] (Fig. 2). The PDGF-BB spectrum indicated the presence of an intense peak at 1641 cm^{-1} and a weak signal at 1549 cm^{-1}, both related to protein amide bands [66]. The PA-6/SOMA nanomembrane loaded with PDGF-BB demonstrated some unique bands that were absent in the pure PA-6/SOMA spectrum.

PDGF-BB is a diffusible signaling protein mediator, essential for a successful tissue repair throughout the three phases of wound healing [14]. The pharmacological activity of rhPDGF-BB is similar to the naturally released PDGF and comprises the promotion of chemotactic recruitment, the formation of granulation tissue and cell proliferation [67]. The rhPDGF-BB gel (becaplermin) is the only currently approved growth factor therapy for wound healing [68]. The tissue repair mechanisms induced by PDGF-BB appear to involve fibroblast proliferation, collagen production, and neovessel formation.

Clinical efficacy has been demonstrated in several phase III studies [69], and the combined results suggest that topical application of PDGF-BB is safe and well tolerated. The binding capability of growth factor interaction with scaffold is critical for preserving and achieving maximal bioactivity, which has been a relatively less emphasized issue in previous studies [70]. One of the major obstacles is the peptides which are either quickly degraded by proteases or removed by exudate before reaching the wound bed [71]. Although numerous covalent immobilization strategies have been proposed, specificity of the coupling site on the growth factors is difficult to achieve, and proteins lose their functionality during the coupling process.

More interestingly, in this set of experiments, PA-6/SOMA nanofiber scaffolds can interact with the growth factor noncovalently, not requiring the use of covalent chemistry for the coupling process. This observation is correlated with the surface free energy results (see in Supplementary files, Table S3). Protein binding affinity to a biomaterial is determined by Coulomb forces and van der Waals interactions [72,73], in this specific case, the amine groups of the polyamide and PDGF-BB can interact by hydrogen bonds.

The PDGF-BB delivering from nanofibers consisted of a time-dependent sustained release during 8–12 h until a plateau is reached (Fig. 3). No statistically variation was observed between the release profiles of PA6-COM and PA-6/SOMA samples, although these biomaterials were capable of extending the bioactivity of PDGF-BB for longer when compared to its topical administration on the wound bed. When intravenously injected, PDGF-BB is rapidly cleared by the circulation in < 2 min [74]. So, the local delivery of the growth factor is assumed to be the best choice to achieve clinical success [75]. Since most of the polyamide substrates have a biological origin, their bioactivities may act synergistically with the delivered growth factor in wound regeneration [76]. This release behavior could be advantageous considering the chemotactic effect of PDGF-BB and the benefit of angiogenesis stimulation at the early stages of the wound healing [77,78]. Moreover, prolonging the PDGF-BB delivery to longer time points may not be ideal by curbing the latent differentiation of the regenerating tissue [76]. The safety of PDGF-BB in prolonged application protocols are not yet concluded and the black-box warning persist. In addition, it should be noted that the experiments were performed at 37 °C and pH 6.0. Lowering of pH to a more acidic environment might alter the optimal activity of the proteases, favors the peptides broken down faster than at alkaline pH values [79].

Maybe the release of PDGF-BB from nanofibers could be prolonged by its chemical conjugation with a crosslinking agent, like heparin. However, a sustained growth factor release is only noticeable through high doses of heparin (~10 mg/mL), which would restart the bleeding by disturbing the clot. Regardless of the delivery-manner of PDGF-BB at the injury site, its presence showed some indicators of wound healing, including a positive modulation of collagen III to collagen I replacement (results not shown), which is correlated with scar-free wound and better mechanical resistance of the tissue [80,81]. These findings highlight the phenotypic changes induced by PDGF-BB in resident cells which are linked to the breakdown of old collagen during tissue remodeling [82].

It is too early to predict a mathematical kinetic equation for the release mechanism of PDGF-BB from the surface of polyamide-based nanofibers. It is known that the magnitude and kinetics of protein release may be governed by many parameters, including the amount of growth factor loaded into the scaffold, biomaterial's fluid retention, diameter of the nanofibers and polymer molecular weight, nanoporosity, biomolecule dissolution/diffusion, and biomolecule distribution inside the matrix [63,65,83]. Srikar et al. [83] attribute the release mechanism of compounds from polymer nanofibers to a two-stage process: a solid-state diffusion mechanism preceded by a limited-desorption of the compound from nanopores in the fibers or the outer surface of the fibers in contact with the release media. Efforts are being made to explore better the results obtained so far.

3.3. Interaction of nanomembranes with the 3T3 and VERO cell cultures

The effects of PA-6 and PA-6/SOMA mats were initially evaluated by MTT assay in two distinct cell lines. No significant differences in cell

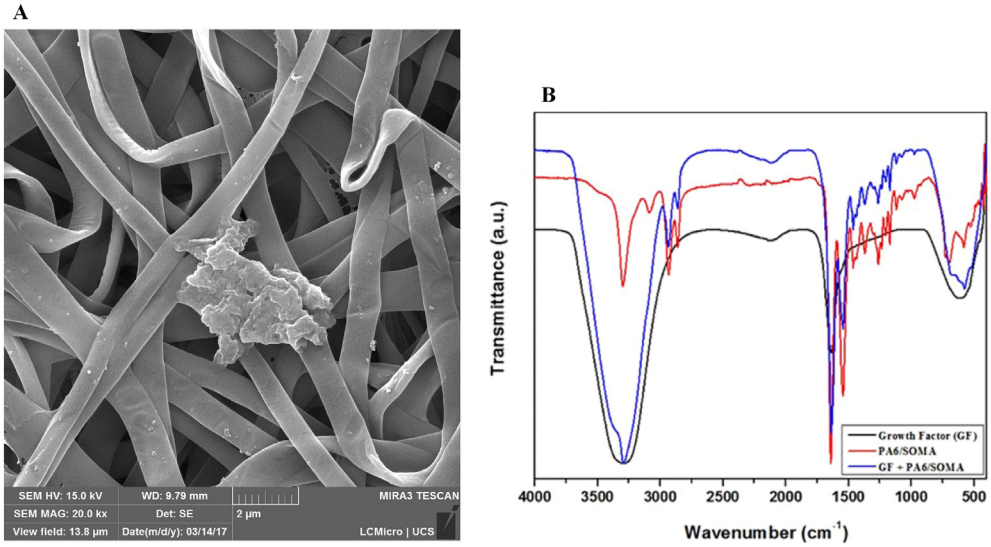

Fig. 2. Evidence of PDGF-BB incorporation into PA-6/SOMA nanomembrane by (A) FEG-SEM (magnification 20.0k×) and (B) FTIR.

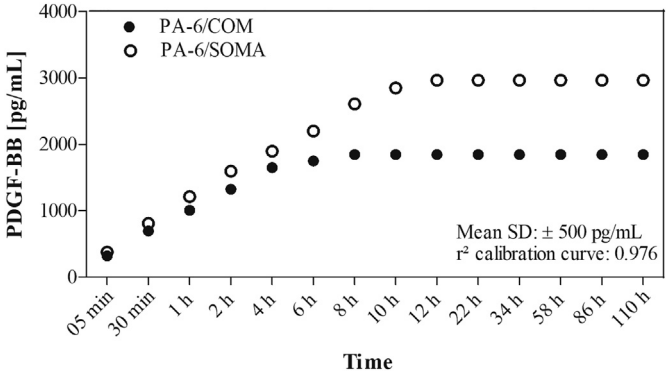

Fig. 3. PDGF-BB release profiles from PA-6 nanomembranes as determined by ELISA.

biocompatibility were observed between commercial PA-6 and PA-6/SOMA nanofibrous scaffolds, as shown in Fig. 4. Neither nanomembrane displayed any cytotoxicity in fibroblast 3T3 and VERO lineages in up to 72 h, denoted that PA-6 and PA-6/SOMA cannot affect the favorable cell environment. Strikingly, insofar these materials induced a promising enhancement of cell viability at 48 h for fibroblast 3T3 lineage, the VERO cells, recommended for screening chemical toxicity *in vitro*, remained viable and able to spread and reproduce. These findings are compatible with the ability to grow and colonize the structure of the materials produced [16].

The cell adhesion affinity by PA-6 and PA-6/SOMA was investigated 24 h post-seeding 3T3 fibroblasts deposited onto the nanofibrillar surfaces (Fig. 5). In the first 24 h of culture, the fibroblast showed a rounded morphology for both nanofibrous mats (4.2 µm; PA-6/SOMA), but adherent contact points with the surrounding fibers and release of ECM by cells could be seen mainly in the PA-6/SOMA sample [84]. 3T3 cells cultured on PA-6/SOMA appeared healthy and exhibited a well-spread and elongated morphology (6.4 µm; PA-6/SOMA) in comparison with fibroblasts grown on PA-6, with extensive projections after 72 h, indicating favorable cell adhesion and migration toward the PA-6/SOMA nanomembrane [53,85].

The cells spread over the fibers by cytoplasmic extensions. This morphology is consistent with a classical *in vivo*-like fibroblast phenotype [86]. The images show that the adhered cells stretched more easily and deposited more ECM across the random SOMA-containing scaffold, better than cells on the pristine PA-6 scaffolds. This behavior confirms the surface free energy results, which revealed an increased adhesiveness to the PA-6/SOMA surface (see in Supplementary files, Table S3). The PA-6/SOMA scaffold structure accelerated the adhesion and the proliferation rates of 3T3 fibroblast cells. The higher percentage of cells that attached to SOMA-containing scaffold could be in part explained by the influence of the surface's polar character, which leads to an enhancement of fibroblast attachment [59,87].

Regarding distinct cell types driven by different cues, Lukyanova et al. [88] reported that non-toxic compounds like soybean oil induce a microenvironment which favors osteoblastic cell migration. The proliferation of preosteoblastic cells on polymeric soybean oil-g-polystyrene membranes was enhanced by the increased soybean oil content [89]. The bioactivity of soybean-based biomaterials favored the osteoblast differentiation *in vitro* and bone repair *in vivo* in rabbit models [90]. Promising cells adhesion and growth were also observed in L-929 from mouse connective tissue when exposed to soybean oil-based polyurethane networks [91]. On the other hand, interesting research headed by Xie et al. [92] suggested an antiproliferative effect in mouse keratinocytes through the use of soy-derived phosphatidylglycerol. This proposal opens new insights into the treatment of different skin diseases, characterized by excessive or insufficient proliferation.

Distinct PA6-blended scaffolds have been prepared and investigated to enhance the cytocompatibility of PA-6 to support treatments for a wide variety of pathologies. A biphasic scaffold composite of PVA/Gel/V-n-HA/PA6 was favorable to BMSCs integration and promoted osteochondral regeneration when applied *in situ* to an osteochondral defect [93]. Treating osteochondral defects is challenging since the interfacial tissue between bone and cartilage has different biological cues to regenerate. The manufactured bi-layered scaffold PVA/Gel/V-n-HA/PA6 supported different abilities of the native osteochondral unit and fulfilled the requirements to integrate the newly formed osteochondral matrix with the surrounding tissues. Nanofiber scaffolds fabricated from PA6–12 have been used to hold growth and proliferation of different stem cells sources. Zajicova et al. [94] chose such a copolyamide as a matrix for the growth of corneal epithelial and endothelial cell lines. The PA6–12 scaffolds supplied the growth of adult-tissue specific cells and their transfer to treat ocular surface injuries. Cytocompatibility properties of polyamide-6/poly(ε-caprolactone) (PA-6/PCL) blend scaffolds were investigated using EA.hy926 human endothelial cells [95]. PA-6 has been engineered to retain mechanical strength and durability in a tissue scaffold. Fibrous scaffolds prepared from different weight ratios of PA-6/PCL blends proved to be an excellent endothelial cell carrier and exhibited promising morphological features, relevant to

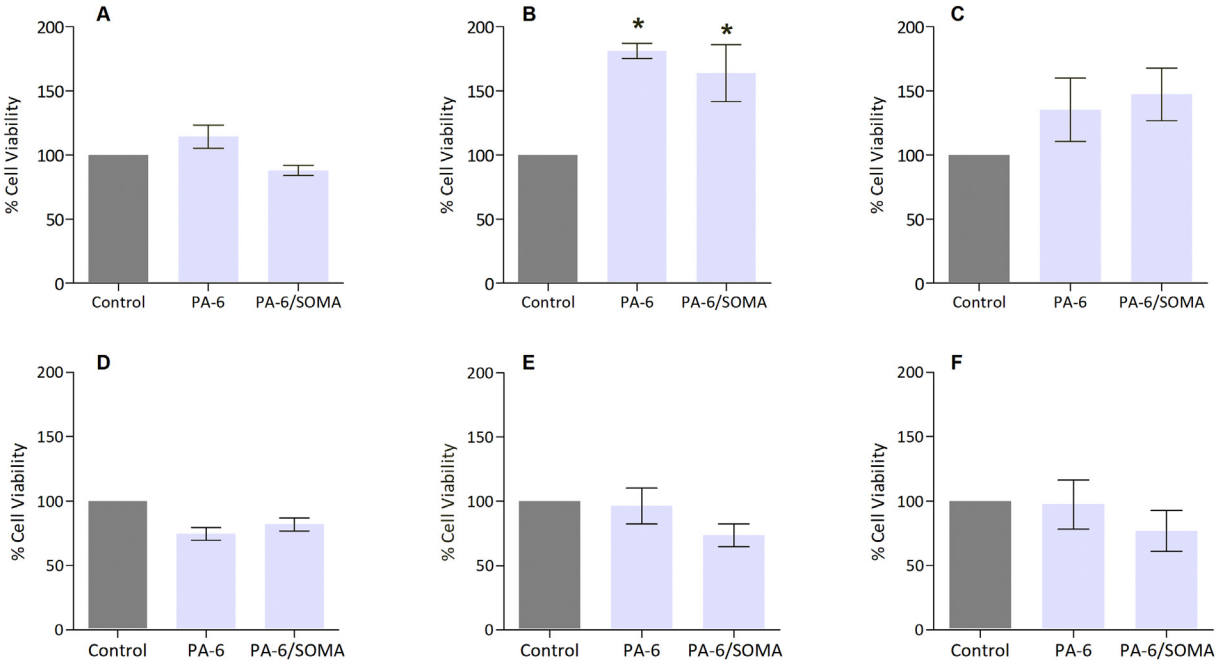

Fig. 4. Effect of incubation with PA-6 and PA-6/SOMA nanomembranes on cell viability of 3T3 murine fibroblast cells after (A) 24 h, (B) 48 h and (C) 72 h and VERO cells after (D) 24 h, (E) 48 h and (F) 72 h. The experiments were carried out at least three times in triplicate. Each column represents the mean ± SEM. $^{*}p < 0.05$ *versus* control.

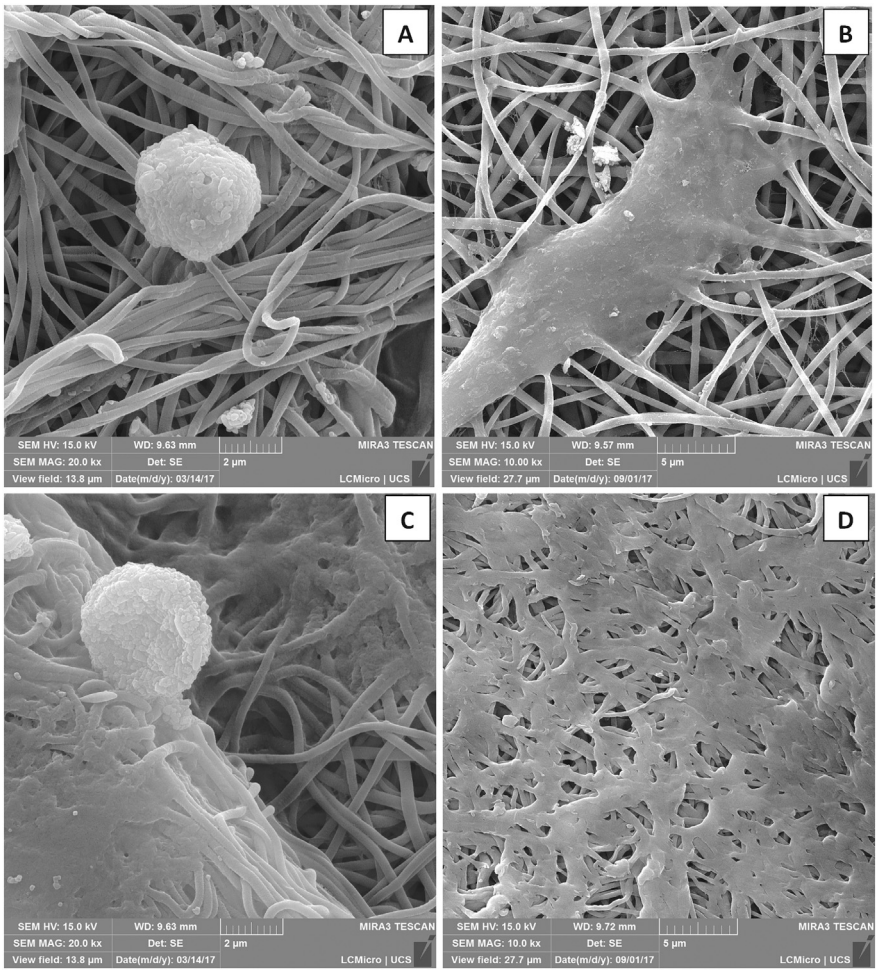

Fig. 5. Fibroblast 3T3 adhesion in (A) commercial PA-6, 24 h; (B) PA-6/SOMA, 24 h; (C) commercial PA-6, 72 h; (D) PA-6/SOMA, 72 h (FEG-SEM magnification 10.0k×; 20.0k×).

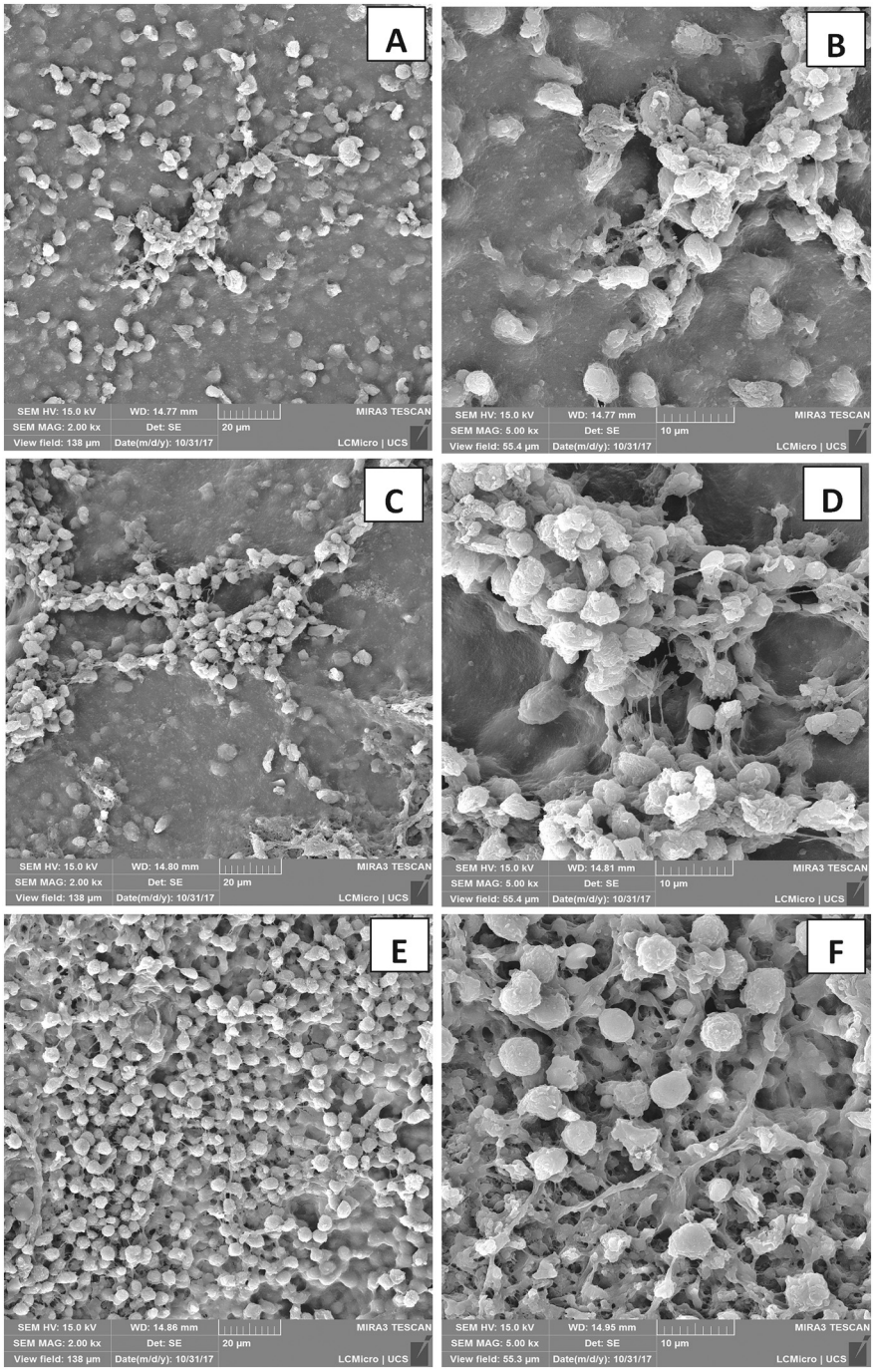

Fig. 6. FEG-SEM analysis of (A, B) commercial PA-6; (C, D) PA-6/SOMA and (E, F) PA-6/SOMA loaded with PDGF-BB nanomembrane behavior in direct contact with the wound 72 h after application (FEG-SEM magnification 2.0k×; 5.0k×).

peripheral blood vessel materials.

3.4. Interaction of nanomembranes with the in vivo wound microenvironment

The behavior of nanomembranes in direct contact with the wound microenvironment was assessed in the first 72 h after application. The PA-6 and PA-6/SOMA scaffolds were analyzed, whether or not loaded with PDGF-BB. The biomaterials remained fixed at the wound site the entire time, without the need of sutures to attach them in position. The ease of handling while the covering was applied and the ability to adhere and conform to the wound surface were mechanical characteristics that were noteworthy [40]. Wound coverings need an ideal structure: one that offers high porosity and provides a good barrier. Such mechanical properties suggest that the PA-6 and PA-6/SOMA nanofiber scaffolds realistically mimic the mechanical characteristics of the soft tissue. The porous structure of electrospun fibrous mats could also absorb excess exudates, confirming the fluid uptake capacity results (see in Supplementary files, Fig. S3) [6].

The biomaterial surface removed from the wound bed after 72 h in direct contact was observed by FEG-SEM (Fig. 6). The microscopic images revealed a more pronounced cellular proliferation, collagen fibrils formation and remarkable ECM secretion for the PA-6/SOMA loaded with PDGF-BB. The ECM confers resistance to the injured histological tissue [96,97]. Collagen fiber is the framework of the dermis, and a healing wound is mainly a result of the net deposition and

stabilization of collagen in the wound area providing strength and protecting it from traumatic damage [6,97].

Thus, collagen formation is a determinant event in the physiological healing process, causing pathological consequences when deficient deposition or alteration of the degradation rates is observed [96]. The presence of a variety of dermal cell phenotypes on nanofiber mats was detected on the 3rd postoperative day [98]. Over time, the biomaterials should be populated by crucial factors and other connective-tissue cells typical of the healthy skin wound microenvironment. The signs of biological events were less expressive in the commercial PA-6 nanomembrane. Cells grown on the pristine PA-6 nanofibers were not well-spread across the surface and raised as a non-continuous monolayer (Fig. 6). In contrast, the cells seeded on the PA-6/SOMA samples had a dendritic appearance with extensions [53]. As expected, PA-6/SOMA loaded with PDGF-BB performed best in attracting cells and intensified the proliferation rates of the different cell types that comprise the wound microenvironment, with more collagen content and ECM deposition (Fig. 6). Several animal studies had demonstrated accelerated wound closure in normal and pathophysiological states when the wound bed was supplemented with exogenous PDGF [99].

3.5. *In vivo* wound-healing assay: macroscopic observation of the wound-healing process

The PA-6/SOMA nanomembranes have presented excellent biocompatibility with the wound microenvironment, dimensional homology to the natural components of ECM and adequate properties to promote the attachment of biomolecules and attract cell types present in the healing phases. At the time, the cutaneous lesion was also evaluated *in vivo* through 14 day post-wounding. The nanofibrous materials were biocompatible and did not cause any local inflammatory reaction in a macroscopic *in vivo* evaluation. Fig. 7 shows the macroscopic observation of the cutaneous healing evolution after treatment with fibrous mats, using an untreated wound as the control. For all groups wounds were observed with serosanguineous crust formation adhered to the injury site after a particular time, including the groups treated with the biomaterials. The cells can secrete proteins that induce the creation of a fibrous capsule around the implanted biomaterial. The nanofiber mats behaved as an interfacial tissue, being encompassed by the fresh tissue formed. As new granulation tissue is being generated, the wound contracts [11].

The wounds that did not receive the biomaterial treatment developed granulation tissue on the 3rd-day post procedure. Early granulation tissue formation also signified autolytic debridement of wound exudates, restricted tissue necrosis, and shortened inflammatory phase [5]. However, no macroscopical differences were observed between the wound contraction rates for all groups at the specified times. The wound closure of the animals was not significantly accelerated by the nanofibrous scaffolds in both the absence and presence of growth factor within a 14-day follow-up. On the other hand, the physical strength generated by the biomaterial application on the wound site did not preclude the wound contraction, which is a good sign. These results do not exclude the possibility that the nanomembranes are capable of modulating other healing parameters at the cellular level.

Karim et al. [100] firstly reported the epithelialization of the skin over a polymeric scaffold in three illustrative cases of patients. The polymeric structure provided a surface for epithelial regeneration and secondary wound closure. In a six-week period, the wound shrank with healthy granulation tissue covering the implanted material, followed by epithelialization and complete closure of the defect with no discharge. At 5-year follow-up, the patients were fully ambulatorial with no clinical signs of infection. Five patients with different causes of burn injury were treated with a dermal scaffold based on PEGT/PBT copolymer [101]. In the same way as polyamide, this copolymer also slowly degrades. One-year post-treatment, intracellular fragments (size up to 100 μm) of the PEGT/PBT copolymer were observed by SEM, indicating that cells were able to phagocytize it. Finally, histological studies are in progress to further investigate the role of PA-6 and PA-6/SOMA in all phases of the wound healing process. It is an attempt to suggest that strict *in vivo* animal modeling, including degradation performance and toxicity studies, should be investigated in future on this class of synthetic polymers to evaluate their suitability for human use.

4. Conclusions

The results indicated that the bioengineered polyamide-6 and soy-modified-based nanomembranes have outstanding biocompatibility and suitable properties to be applied as a platform to active carrier biomolecules and to support cellular adhesion as well as the development of new functional tissues. The nanofibrous scaffolds showed a dimensional homology to natural ECM components and promoted the attachment of 3T3 fibroblast cells in addition to promote cell proliferation. Besides, the incorporation of PDGF-BB growth factor in polyamide nanofibers sustained the peptide bioactivity. Mechanically,

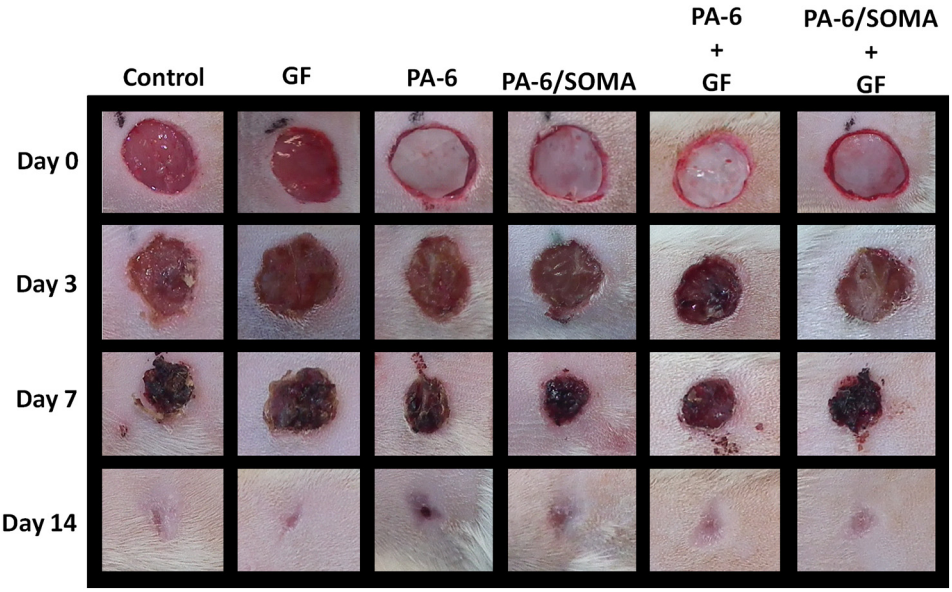

Fig. 7. Representative images of wounds over the course of the healing process on days 0, 3, 7 and 14. Scale bar = 10 mm.

the nanomembranes were able to withstand the sterilization process and to conform adequately to the wound surface. The chemical modification of PA-6 chains with a fatty acid (soybean) derivative led to an increase of surface free energy, which favored cell adhesiveness, collagen formation, and ECM secretion. The remarkable fluid retention capacity should be considered as a positive property that allowed the easy adherence, maintained a moist environment to modulate the autolytic debridement and prevented the excess of exudate on the wound bed. No side effects were observed in a macroscopic *in vivo* evaluation of the wound site. Although the nanomembranes have not accelerated the wound closure of the animals during the 14 day follow-up, their potential of modulating other healing parameters at a cellular and histological levels cannot be excluded. Compared to currently available dermal dressings for skin regeneration, these materials have the added advantages of being ultra-thin, more easily handled and better integrated to host-tissue, requiring minimal wound management. The development and use of nylon-based coverings have been encouraged primarily by the United States Army for combat applications as well as mass casualty situations.

Conflict of interest

The authors declare that they have no conflict of interest.

Acknowledgements

The authors thank “Mantova Industria de tubos flexíveis” for donating the polyamide and CAPES for the scholarship to Fernanda Dias and Lucas Dall Agnol. This work was supported by National Council for Scientific and Technological Development (CNPq), Brazil (Grants 308241/2015-0). The authors also thank the Brazilian Synchrotron Light Laboratory (LNLS) for the use of their scientific installations (SAXS1 beamline).

Authorship contributions

F.T.G.D., N.F.N. and, O.B. designed the experiments, analyzed the data and wrote the manuscript; A.R.I. contributed in *in vivo* experiments; F.C.M. supported and produced membranes used; L.D. assisted in surface energy characterization; D.R.M. and J.C.C. provided cell culture facilities and contributed in *in vitro* experiments; A.F., J.C.C. and R.M.D.S. made a critical review of the manuscript.

Appendix A. Supplementary data

Supplementary data to this article can be found online at https://doi.org/10.1016/j.msec.2019.02.019.

References

[1] P.S. Murphy, G.R.D. Evans, Advances in wound healing: a review of current wound healing products, Plast. Surg. Int. (2012) 190436, , https://doi.org/10.1155/2012/190436 (1–8).
[2] E.A.T. Vargas, N.C.V. Baracho, J. Brito, A.A.A. Queiroz, Hyperbranched polyglycerol electrospun nanofibers for wound dressing applications, Acta Biomater. 6 (2010) 1069–1078, https://doi.org/10.1016//j.actbio.2009.09.018.
[3] E. Boughton, S.V. Mclennan, Biomimetic scaffolds for skin tissue and wound repair, in: A.J. Ruys (Ed.), Biomimetic Biomaterials - Structure and Applications, Woodhead Publishing Series in Biomaterials, 2013, pp. 153–180.
[4] A. Aurora, A. Beasy, J.A. Rizzo, K.K. Chung, The use of a silver–nylon dressing during evacuation of military burn casualties, J. Burn Care Res. 39 (2018) 593–597, https://doi.org/10.1093/jbcr/irx026.
[5] P. Pal, P. Dadhich, P.K. Srivas, B. Das, D. Maulik, S. Dhara, Bilayered nanofibrous 3D hierarchy as skin rudiment by emulsion electrospinning for burn wound management, Biomater. Sci. 5 (2017) 1786–1799, https://doi.org/10.1039/C7BM00174F.
[6] Y. Yang, T. Xia, F. Chen, W. Wei, C. Liu, S. He, X. Li, Electrospun fibers with plasmid bFGF polyplex loadings promote skin wound healing in diabetic rats, Mol. Pharm. 9 (2012) 48–58, https://doi.org/10.1021/mp200246b.
[7] J. Xie, B. Ma, Nanofiber scaffolds and methods for repairing skin damage, US20140004159A1 patent, Marshall University Research Corporation, 2014.
[8] D.G. Murray, Burn wound dressing material, US4767619A patent, 1988, 10p.
[9] K.M. Kennedy, A. Bhaw-Luximon, D. Jhurry, Skin tissue engineering: biological performance of electrospun polymer scaffolds and translational challenges, Regen. Eng. Transl. Med. 3 (2017) 201–214, https://doi.org/10.1007/s40883-017-0035-x.
[10] S. Canonico, F. Campitiello, A. Della Corte, V. Padovano, G. Pellino, Treatment of leg chronic wounds with dermal substitutes and thin skin grafts, in: M. Gore (Ed.), Skin Grafts, IntechOpen, 2013, pp. 51–76, , https://doi.org/10.5772/51852.
[11] K.A. Rieger, N.P. Birch, J.D. Schiffman, Designing electrospun nanofiber mats to promote wound healing – a review, J. Mater. Chem. B 1 (2013) 4531–4541, https://doi.org/10.1039/C3TB20795A.
[12] M. Liu, X.-P. Duan, Y.-M. Li, D.-P. Yang, Y.-Z. Long, Electrospun nanofibers for wound healing, Mater. Sci. Eng. C 76 (2017) 1413–1423, https://doi.org/10.1016/j.msec.2017.03.034.
[13] Y.Z. Zhang, J. Venugopal, Z.-M. Huang, C.T. Lim, S. Ramakrishna, Characterization of the surface biocompatibility of the electrospun PCL-collagen nanofibers using fibroblasts, Biomacromolecules 6 (2005) 2583–2589, https://doi.org/10.1021/bm050314k.
[14] J.K. Choi, J.-H. Jang, W.-H. Jang, J. Kim, I.-H. Bae, J. Bae, Y.-H. Park, B.-J. Kim, K.-M. Lim, J.-W. Park, The effect of epidermal growth factor (EGF) conjugated with low-molecular-weight protamine (LMWP) on wound healing of the skin, Biomaterials 33 (2012) 8579–8590, https://doi.org/10.1016/j.biomaterials.2012.07.061.
[15] I. Garcia-Orue, G. Gainza, F.B. Gutierrez, J.J. Aguirre, C. Evora, J.L. Pedraz, R.M. Hernandez, A. Delgado, M. Igartua, Novel nanofibrous dressings containing rhEGF and Aloe vera for wound healing applications, Int. J. Pharm. 523 (2017) 556–566, https://doi.org/10.1016/j.ijpharm.2016.11.006.
[16] A.R. Unnithan, N.A.M. Barakat, P.B.T. Pichiah, G. Gnanasekaran, R. Nirmala, Y.-S. Cha, C.-H. Jung, M. El-Newehy, H.Y. Kim, Wound-dressing materials with antibacterial activity from electrospun polyurethane–dextran nanofiber mats containing ciprofloxacin HCl, Carbohydr. Polym. 90 (2012) 1786–1793, https://doi.org/10.1016/j.carbpol.2012.07.071.
[17] H. Chen, Y. Peng, S. Wu, L.P. Tan, Electrospun 3D fibrous scaffolds for chronic wound repair, Materials 9 (2016) 272–283, https://doi.org/10.3390/ma9040272.
[18] A.B. Tekinay, M.O. Guler, D. Mumcuoglu, S. Ustun, Peptide nanofibers for controlled growth factor release, Ther. Deliv. 4 (2013) 651–654, https://doi.org/10.4155/tde.13.35.
[19] V. Delplace, J. Nicolas, Degradable vinyl polymers for biomedical applications, Nat. Chem. 7 (2015) 771–784, https://doi.org/10.1038/nchem.2343.
[20] B. Joseph, A. George, S. Gopi, N. Kalarikkal, S. Thomas, Polymer sutures for simultaneous wound healing and drug delivery - a review, Int. J. Pharm. 524 (2017) 454–466, https://doi.org/10.1016/j.ijpharm.2017.03.041.
[21] J.A. Hudson, A. Crugnola, The in vivo biodegradation of nylon 6 utilized in a particular IUD, J. Biomater. Appl. 1 (1987) 487–501.
[22] M.S. Marqués, C. Regaño, J. Nyugena, L. Aidanpa, S. Muñoz-Guerra, Hydrolytic and fungal degradation of polyamides derived from tartaric acid and hexamethylenediamine, Polymer 41 (2000) 2765–2772, https://doi.org/10.1016/S0032-3861(99)00422-X.
[23] C.S. Proikakis, N.J. Mamouzelos, P.A. Tarantili, A.G. Andreopoulos, Swelling and hydrolytic degradation of poly(D,L-lactic acid) in aqueous solutions, Polym. Degrad. Stab. 91 (2006) 614–619, https://doi.org/10.1016/j.polymdegradstab.2005.01.060.
[24] I. Tocco, B. Zavan, F. Bassetto, V. Vindigni, Nanotechnology-based therapies for skin wound regeneration, J. Nanomater. (2012) 1–11, https://doi.org/10.1155/2012/714134.
[25] A. Schneider, X.Y. Wang, D.L. Kaplan, J.A. Garlick, C. Egles, Biofunctionalized electrospun silk mats as a topical bioactive dressing for accelerated wound healing, Acta Biomater. 5 (2009) 2570–2578, https://doi.org/10.1016/j.actbio.2008.12.013.
[26] D. Egozi, M. Baranes-Zeevi, Y. Ullmann, A. Gilhar, A. Keren, E. Matanes, I. Berdicevsky, N. Krivoy, M. Zilberman, Biodegradable soy wound dressings with controlled release of antibiotics: results from a guinea pig burn model, Burns 41 (2015) 1459–1467, https://doi.org/10.1016/j.burns.2015.03.013.
[27] M. Límová, Active wound coverings: bioengineered skin and dermal substitutes, Surg. Clin. North Am. 90 (2010) 1237–1255, https://doi.org/10.1016/j.suc.2010.08.004.
[28] P. Aramwit, Introduction to biomaterials for wound healing, in: M. Ågren (Ed.), Wound Healing Biomaterials, Woodhead Publishing, 2016, pp. 3–38, , https://doi.org/10.1016/B978-1-78242-456-7.00001-5.
[29] S. Chattopadhyay, R. Raines, Review collagen-based biomaterials for wound healing, Biopolymers 101 (2014) 821–833, https://doi.org/10.1002/bip.22486.
[30] R.W.C. Morris, Mepitel: a non-adherent wound dressing with Safetac technology, Br. J. Nurs. 18 (2009) 58–64, https://doi.org/10.12968/bjon.2009.18.1.93582.
[31] J. Terron, J. Codina, M.D.P.d. Caz, J. Safont, V. Mirabet, A biosynthetic skin substitute (biobrane) in the management of burns, J. Euro-Mediterr. Counc. Burns Fire Disasters 8 (1995) 1–5.
[32] J.R. Ernzen, F. Bondan, C. Luvison, C.H. Wanke, J.D.-N. Martins, R. Fiorio, O. Bianchi, Structure and properties relationship of melt reacted polyamide 6/malenized soybean oil, J. Appl. Polym. Sci. 133 (2016) 10, https://doi.org/10.1002/app.43050.
[33] C.T. Rueden, J. Schindelin, M.C. Hiner, B.E. DeZonia, A.E. Walter, E.T. Arena, K.W. Eliceiri, ImageJ2: ImageJ for the next generation of scientific image data, BMC Bioinforma. 18 (2017) 529–555, https://doi.org/10.1186/s12859-017-1934-z.
[34] M. Kłonica, J. Kuczmaszewski, M.P. Kwiatkowski, J. Ozonek, Polyamide 6 surface

layer following ozone treatment, Int. J. Adhes. Adhes. 64 (2016) 179–187, https://doi.org/10.1016/j.ijadhadh.2015.10.017.
[35] U. Stachewicz, A.H. Barber, Enhanced wetting behavior at electrospun polyamide nanofiber surfaces, Langmuir 27 (2011) 3024–3029, https://doi.org/10.1021/la1046645.
[36] L.E. Nita, A.P. Chiriac, E. Stoleru, A. Diaconu, N. Tudorachi, Tailorable polyelectrolyte protein complex based on poly(aspartic acid) and bovine serum albumin, Des. Monomers Polym. 19 (2016) 596–606, https://doi.org/10.1080/15685551.2016.1187436.
[37] J. Comyn, Contact angles in the study of adhesion, Adhesion Science, Royal Society of Chemistry, Cambridge, 2007, pp. 98–113, , https://doi.org/10.1039/9781847550064-00098.
[38] ISO-10993-5, Biological evaluation of medical devices. Part 5: tests for in vitro cytotoxicity, in: T.I.O.f. Standardization (Ed.), ISO 10993-5:2009(E), 2009, p. 42.
[39] M. Abrigo, S.L. McArthur, P. Kingshott, Electrospun nanofibers as dressings for chronic wound care: advances, challenges, and future prospects, Macromol. Biosci. 14 (2014) 772–792, https://doi.org/10.1002/mabi.201300561.
[40] E.Z. Cai, E.Y. Teo, L. Jing, Y.P. Koh, T.S. Qian, F. Wen, J.W.K. Lee, E.C.H. Hing, Y.L. Yap, H. Lee, C.N. Lee, S.-H. Teoh, J. Lim, T.C. Lim, Bio-conjugated polycaprolactone membranes: a novel wound dressing, Arch. Plast. Surg. 41 (2014) 638–646, https://doi.org/10.5999/aps.2014.41.6.638.
[41] Y. Liu, L. Cui, F. Guan, Y. Gao, N.E. Hedin, L. Zhu, H. Fong, Crystalline morphology and polymorphic phase transitions in electrospun nylon-6 nanofibers, Macromolecules 40 (2007) 6283–6290, https://doi.org/10.1021/ma070039p.
[42] M. Richard-Lacroix, C. Pellerin, Molecular orientation in electrospun fibers: from mats to single fibers, Macromolecules 46 (2013) 9473–9493, https://doi.org/10.1021/ma401681m.
[43] J.S. Stephens, D.B. Chase, J.F. Rabolt, Effect of the electrospinning process on polymer crystallization chain conformation in nylon-6 and nylon-12, Macromolecules 37 (2004) 877–881, https://doi.org/10.1021/ma0351569.
[44] M. Gazzano, C. Gualandi, A. Zucchelli, T. Sui, A.M. Korsunsky, C. Reinhard, M.L. Focarete, Structure-morphology correlation in electrospun fibers of semicrystalline polymers by simultaneous synchrotron SAXS-WAXD, Polymer 63 (2015) 154–163, https://doi.org/10.1016/j.polymer.2015.03.002.
[45] E. Marsano, L. Francis, F. Giunco, Polyamide 6 nanofibrous nonwovens via electrospinning, J. Appl. Polym. Sci. 117 (2010) 1754–1765, https://doi.org/10.1002/app.32118.
[46] R. Nirmala, R. Navamathavan, M.H. El-Newehy, H.Y. Kim, Preparation and characterization of electrospun ultrafine polyamide-6 nanofibers, Polym. Int. 60 (2011) 1475–1480, https://doi.org/10.1002/pi.3105.
[47] S.-Y. Tsou, H.-S. Lin, C. Wang, Studies on the electrospun nylon 6 nanofibers from polyelectrolyte solutions: 1. Effects of solution concentration and temperature, Polymer 52 (2011) 3127–3136, https://doi.org/10.1016/j.polymer.2011.05.010.
[48] B.P. Grady, Simple SAXS and WAXS software written in Excel, http://coecs.ou.edu/Brian.P.Grady/saxssoftware.html (Oklahoma).
[49] J.M. Samon, J.M. Schultz, B.S. Hsiao, Study of the cold drawing of nylon 6 fiber by in-situ simultaneous small- and wide-angle X-ray scattering techniques, Polymer 41 (2000) 2169–2182, https://doi.org/10.1016/S0032-3861(99)00378-X.
[50] M. Omer, T. Kamal, H.-H. Cho, D.-K. Kim, S.-Y. Park, Preparation and structure of nylon 4/6 random-copolymer nanofibers, Macromol. Res. 20 (2012) 810–815, https://doi.org/10.1007/s13233-012-0121-3.
[51] M.T. McClendon, S.I. Stupp, Tubular hydrogels of circumferentially aligned nanofibers to encapsulate and orient vascular cells, Biomaterials 33 (2012) 5713–5722, https://doi.org/10.1016/j.biomaterials.2012.04.040.
[52] E. Zussman, M. Burman, A.L. Yarin, R. Khalfin, Y. Cohen, Tensile deformation of electrospun nylon-6,6 nanofibers, J. Polym. Sci. B Polym. Phys. 44 (2006) 1482–1489, https://doi.org/10.1002/polb.20803.
[53] A. Abdal-hay, L.D. Tijing, J.K. Lim, Characterization of the surface biocompatibility of an electrospun nylon 6/CaP nanofiber scaffold using osteoblasts, Chem. Eng. J. 215–216 (2013) 57–64, https://doi.org/10.1016/j.cej.2012.10.046.
[54] A.A. Spector, K. John, J.E. Fletcher, Binding of long-chain fatty acids to bovine serum albumin, J. Lipid Res. 10 (1969) 56–67.
[55] M. Arhanta, P.-Y. Le Gac, M. Le Gall, C. Burtin, C. Briançon, P. Davies, Modelling the non Fickian water absorption in polyamide 6, Polym. Degrad. Stab. 133 (2016) 404–412, https://doi.org/10.1016/j.polymdegradstab.2016.09.001.
[56] G. Dlubek, F. Redmann, R. Krause-Rehberg, Humidity-induced plasticization and antiplasticization of polyamide-6: a positron life-time study of the local free volume, J. Appl. Polym. Sci. 84 (2002) 244–255, https://doi.org/10.1002/app.10319.
[57] V. Miri, O. Persyn, J.-M. Lefebvre, R. Seguela, Effect of water absorption on the plastic deformation behavior of nylon 6, Eur. Polym. J. 45 (2009) 757–762, https://doi.org/10.1016/j.eurpolymj.2008.12.008.
[58] A.H. Hekmati, N. Khenoussi, H. Nouali, J. Patarin, J.-Y. Drean, Effect of nanofiber diameter on water absorption properties and pore size of polyamide electrospun-6 nanoweb, Text. Res. J. 84 (2014) 2045–2055, https://doi.org/10.1177/0040517514532160.
[59] S.E. Kim, D.N. Heo, J.B. Lee, J.R. Kim, S.H. Park, S.H. Jeon, I.K. Kwon, Electrospun gelatin/polyurethane blended nanofibers for wound healing, Biomed. Mater. 4 (2009), https://doi.org/10.1088/1748-6041/4/4/044106 (12 pp.).
[60] P. Zahedi, Z. Karami, I. Rezaeian, S.-H. Jafari, P. Mahdaviani, A.H. Abdolghaffari, M. Abdollahi, Preparation and performance evaluation of tetracycline hydrochloride loaded wound dressing mats based on electrospun nanofibrous poly(lactic acid)/poly(e-caprolactone) blends, J. Appl. Polym. Sci. 124 (2012) 4174–4183, https://doi.org/10.1002/app.35372.
[61] M. Sadri, A. Mohammadi, H. Hosseini, Drug release rate and kinetic investigation of composite polymeric nanofibers, Nanomed. Res. J. 1 (2016) 112–121, https://doi.org/10.7508/NMRJ.2016.02.008.
[62] L.L.L. Benskin, PolyMem® Wic® Silver® rope: a multifunctional dressing for decreasing pain, swelling, and inflammation, Adv. Wound Care 1 (2012) 44–47, https://doi.org/10.1089/wound.2011.0285.
[63] H. Zigdon-Giladi, A. Khutaba, R. Elimelech, E.E. Machtei, S. Srouji, VEGF release from a polymeric nanofiber scaffold for improved angiogenesis, J. Biomed. Mater. Res. A 105 (2017) 2712–2721, https://doi.org/10.1002/jbm.a.36127.
[64] S. Hampton, A small study in healing rates and symptom control using a new sheet hydrogel dressing, J. Wound Care 13 (2004) 297–300, https://doi.org/10.12968/jowc.2004.13.7.26639.
[65] S. Sahoo, L.T. Ang, J.C.-H. Goh, S.-L. Toh, Growth factor delivery through electrospun nanofibers in scaffolds for tissue engineering app, J. Biomed. Mater. Res. A 93A (2010) 1539–1550, https://doi.org/10.1002/jbm.a.32645.
[66] L.J. Reigstad, H.M. Sande, O. Fluge, O. Bruland, A. Muga, J.E. Varhaug, A. Martínez, J.R. Lillehaug, Platelet-derived growth factor (PDGF)-C, a PDGF family member with a vascular endothelial growth factor-like structure, J. Biol. Chem. 278 (2003) 17114–17120, https://doi.org/10.1074/jbc.M301728200.
[67] G.R. Grotendorst, G.R. Martin, D. Pencev, J. Sodek, A.K. Harvey, Stimulation of granulation tissue formation by platelet-derived growth factor in normal and diabetic rats, J. Clin. Invest. 76 (1985) 2323–2329, https://doi.org/10.1172/JCI112243.
[68] J. Andrae, R. Gallini, C. Betsholtz, Role of platelet-derived growth factors in physiology and medicine, Genes Dev. 22 (2008) 1276–1312, https://doi.org/10.1101/gad.1653708.
[69] J.M. Smiell, T.J. Wieman, D.L. Steed, B.H. Perry, A.R. Sampson, B.H. Schwab, Efficacy and safety of becaplermin (recombinant human platelet-derived growth factor-BB) in patients with nonhealing, lower extremity diabetic ulcers: a combined analysis of four randomized studies, Wound Repair Regen. 7 (1999) 335–346, https://doi.org/10.1046/j.1524-475X.1999.00335.x.
[70] R. Mammadov, B. Mammadov, M.O. Guler, A.B. Tekinay, Growth factor binding on heparin mimetic peptide nanofibers, Biomacromolecules 13 (2012) 3311–3319, https://doi.org/10.1021/bm3010897.
[71] R. Jain, A. Agarwal, P.R. Kierski, M.J. Schurr, C.J. Murphy, J.F. McAnulty, N.L. Abbott, The use of native chemical functional groups presented by wound beds for the covalent attachment of polymeric microcarriers of bioactive factors, Biomaterials 34 (2013) 340–352, https://doi.org/10.1016/j.biomaterials.2012.09.055.
[72] D.T. Haynie, D.B. Khadka, M.C. Cross, Physical properties of polypeptide electrospun nanofiber cell culture scaffolds on a wettable substrate, Polymers 4 (2012) 1535–1553, https://doi.org/10.3390/polym4031535.
[73] A. Nur-E-Kamal, I. Ahmed, J. Kamal, A.N. Babu, M. Schindler, S. Meiners, Covalently attached FGF-2 to three-dimensional polyamide nanofibrillar surfaces demonstrates enhanced biological stability and activity, Mol. Cell. Biochem. 309 (2008) 157–166, https://doi.org/10.1007/s11010-007-9654-8.
[74] Y.J. Bae, C.H. Cho, W.J. Lee, J.S. Huh, J.O. Lim, Optimization of recombinant human platelet-derived growth factor-BB encapsulated in poly (lactic-co-glycolic acid) microspheres for applications in wound healing, Tissue Eng. Regen. Med. 13 (2016) 13–20, https://doi.org/10.1007/s13770-015-0029-z.
[75] J.O. Hollinger, C.E. Hart, S.N. Hirsch, S. Lynch, G.E. Friedlaender, Recombinant human platelet-derived growth factor: biology and clinical applications, J. Bone Joint Surg. Am. 90 (2008) 48–54, https://doi.org/10.2106/JBJS.G.01231.
[76] P. Koria, Delivery of growth factors for tissue regeneration and wound healing, BioDrugs 26 (2012) 163–175, https://doi.org/10.2165/11631850-000000000-00000.
[77] M.M. Ammar, G.H. Waly, S.H. Saniour, T.A. Moussa, Growth factor release and enhanced encapsulated periodontal stem cells viability by freeze-dried platelet concentrate loaded thermo-sensitive hydrogel for periodontal regeneration, Saudi Dent. J. 30 (2018) 355–364, https://doi.org/10.1016/j.sdentj.2018.06.002.
[78] Z. Xie, C.B. Paras, H. Weng, P. Punnakitikashem, L.-C. Su, K. Vu, L. Tang, J. Yang, K.T. Nguyen, Dual growth factor releasing multi-functional nanofibers for wound healing, Acta Biomater. 9 (2013) 9351–9359, https://doi.org/10.1016/j.actbio.2013.07.030.
[79] A. Ciechanover, Proteolysis: from the lysosome to ubiquitin and the proteasome, Nat. Rev. Mol. Cell Biol. 6 (2005) 79–87 (https://doi.org/1038/nrm1552).
[80] M. Younesi, B.O. Donmez, A. Islam, O. Akkus, Heparinized collagen sutures for sustained delivery of PDGF-BB: delivery profile and effects on tendon-derived cells in-vitro, Acta Biomater. 41 (2016) 100–109, https://doi.org/10.1016/j.actbio.2016.05.036.
[81] H.K. Min, O.S. Kwon, S.H. Oh, J.L. Lee, Platelet-derived growth factor-BB-immobilized asymmetrically porous membrane for enhanced rotator cuff tendon healing, Tissue Eng. Regen. Med. 13 (2016) 568–578, https://doi.org/10.1007/s13770-016-9120-3.
[82] B.M. Hantash, L. Zhao, J.A. Knowles, H.P. Lorenz, Adult and fetal wound healing, Front. Biosci. 13 (2008) 51–61.
[83] R. Srikar, A.L. Yarin, C.M. Megaridis, A.V. Bazilevsky, E. Kelley, Desorption-limited mechanism of release from polymer nanofibers, Langmuir 24 (2008) 965–974, https://doi.org/10.1021/la702449k.
[84] K. Park, Y.M. Ju, J.S. Son, K.-D. Ahn, D.K. Han, Surface modification of biodegradable electrospun nanofiber scaffolds and their interaction with fibroblasts, J. Biomater. Sci. Polym. Ed. 18 (2007) 369–382, https://doi.org/10.1163/156856207780424997.
[85] M.H. El-Newehy, S.S. Al-Deyab, E.-R. Kenawy, A.A. Abdel-Megeed, Nanospider technology for the production of nylon-6 nanofibers for biomedical applications, J. Nanomater. (2011) 626589, , https://doi.org/10.1155/2011/626589 (8 pp.).
[86] M. Schindler, I. Ahmed, J. Kamal, A. Nur-E-Kamal, T.H. Grafe, H.Y. Chung, S. Meiners, A synthetic nanofibrillar matrix promotes in vivo-like organization and

morphogenesis for cells in culture, Biomaterials 26 (2005) 5624–5631, https://doi.org/10.1016/j.biomaterials.2005.02.014.
[87] L. Yang, R.A. Kandel, G. Chang, J.P. Santerre, Polar surface chemistry of nanofibrous polyurethane scaffold affects annulus fibrosus cell attachment and early matrix accumulation, J. Biomed. Mater. Res. A 91 (2009) 1089–1099, https://doi.org/10.1002/jbm.a.32331.
[88] L. Lukyanova, S. Franceschi-Messant, P. Vicendo, E. Pereza, I. Rico-Lattes, R. Weinkamer, Preparation and evaluation of microporous organogel scaffolds for cell viability and proliferation, Colloids Surf. B: Biointerfaces 79 (2010) 105–112 (http://dx.doi.org/1016/j.colsurfb.2010.03.044).
[89] R.S.T. Aydin, B. Hazer, M. Acar, M. Gümüsderelioglu, Osteogenic activities of polymeric soybean oil-g-polystyrene membranes, Polym. Bull. 70 (2013) 2065–2082, https://doi.org/10.1007/s00289-013-0976-2.
[90] M. Santin, L. Ambrosio, Soybean-based biomaterials: preparation, properties and tissue regeneration potential, Expert Rev. Med. Devices 5 (2008) 349–358, https://doi.org/10.1586/17434440.5.3.349.
[91] S. Miao, L. Sun, P. Wang, R. Liu, Z. Su, S. Zhang, Soybean oil-based polyurethane networks as candidate biomaterials: synthesis and biocompatibility, Eur. J. Lipid Sci. Technol. 114 (2012) 1165–1174, https://doi.org/10.1002/ejlt.201200050.
[92] D. Xie, M. Seremwe, J.G. Edwards, R. Podolsky, W.B. Bollag, Distinct effects of different phosphatidylglycerol species on mouse keratinocyte proliferation, PLoS One 9 (2014) 1–9, https://doi.org/10.1371/journal.pone.0107119.
[93] X. Li, Y. Li, Y. Zuo, D. Qu, Y. Liu, T. Chen, N. Jiang, H. Li, J. Li, Osteogenesis and chondrogenesis of biomimetic integrated porous PVA/gel/V-n-HA/pa6 scaffolds and BMSCs construct in repair of articular osteochondral defect, J. Biomed. Mater. Res. A 103 (2015) 3226–3236, https://doi.org/10.1002/jbm.a.35452.
[94] A. Zajicova, K. Pokorna, A. Lencova, M. Krulova, E. Svobodova, S. Kubinova, E. Sykova, M. Pradny, J. Michalek, J. Svobodova, M. Munzarova, V. Holan, Treatment of ocular surface injuries by limbal and mesenchymal stem cells growing on nanofiber scaffolds, Cell Transplant. 19 (2010) 1281–1290, https://doi.org/10.3727/096368910X509040.
[95] A. Abdal-hay, K.A. Khalil, F.F. Al-Jassir, A.M. Gamal-Eldeen, Biocompatibility properties of polyamide 6/PCL blends composite textile scaffold using EA.hy926 human endothelial cells, Biomed. Mater. 12 (2017) 1–12, https://doi.org/10.1088/1748-605X/aa6306.
[96] J.E. Janis, B. Harrison, Wound healing: part I. Basic science, Plast. Reconstr. Surg. 133 (2014) 199–207, https://doi.org/10.1097/01.prs.0000437224.02985.f9.
[97] J.M. Reinke, H. Sorg, Wound repair and regeneration, Eur. Surg. Res. 49 (2012) 35–43, https://doi.org/10.1159/000339613.
[98] L. Lin, A. Perets, Y.-e. Har-el, D. Varma, M. Li, P. Lazarovici, D.L. Woerdeman, P.I. Lelkes, Alimentary 'green' proteins as electrospun scaffolds for skin regenerative engineering, J. Tissue Eng. Regen. Med. 7 (2013) 994–1008, https://doi.org/10.1002/term.1493.
[99] E. Uhl, F. Rösken, A. Sirsjö, K. Messmer, Influence of platelet-derived growth factor on microcirculation during normal and impaired wound healing, Wound Repair Regen. 11 (2003) 361–367, https://doi.org/10.1046/j.1524-475X.2003.11508.x.
[100] K.Z. Masrouha, Y. El-Bitar, M. Najjar, S. Saghieh, Epithelialization over a scaffold of antibiotic impregnated PMMA beads: a salvage technique for open tibial fractures with bone and soft tissue loss when all else fails, Arch. Bone Jt. Surg. 4 (2016) 259–263.
[101] I. Mensik, E.N. Lamme, J. Riesle, P. Brychta, Effectiveness and safety of the PEGT/PBT copolymer scaffold as dermal substitute in scar reconstruction wounds (feasibility trial), Cell Tissue Bank. 3 (2002) 245–253, https://doi.org/10.1023/A:1024674325253.